



Hypoxia-induced and HIF1 α -VEGF-mediated tight junction dysfunction in choriocarcinoma cells: Implications for preeclampsia

Yuan Zhang^{a,1}, Hai-jun Zhao^{a,b,1}, Xin-ru Xia^a, Fei-yang Diao^a, Xiang Ma^a, Jing Wang^a, Li Gao^a, Jie Liu^a, Chao Gao^a, Yu-gui Cui^a, Jia-yin Liu^{a,*}

^a State Key Laboratory of Reproductive Medicine, Center of Clinical Reproductive Medicine, The First Affiliated Hospital of Nanjing Medical University, Nanjing, Jiangsu 210029, China

^b Department of Reproductive Medicine, Central Hospital of Handan City, Handan, Hebei 956000, China

ARTICLE INFO

Keywords:

Tight junction
Hypoxia
Hypoxia-inducible factor 1 alpha
Trophoblast
Preeclampsia

ABSTRACT

Introduction: Accumulated data indicate that placental hypoxia is implicated in the pathogenesis of preeclampsia (PE). Tight junction (TJ) is important structure that sustains normal placental barrier function, its dysregulation under hypoxia has been observed. This study was designed to explore hypoxia-induced TJ dysfunction in trophoblast cells and its possible involvement in PE pathophysiology.

Methods: Choriocarcinoma cells were grown in a monolayer and treated with cobalt chloride (CoCl₂) to induce hypoxia. TJ architecture was assessed using transmission electron microscopy, and locations of TJ proteins were determined by immunofluorescence. TJ functions were assessed by transepithelial electrical resistance (TER) and increased cell paracellular permeability (CPP), and the expression of TJ-related proteins, HIF-1 α and VEGF was measured.

Results: The TJ functions of trophoblast cells were significantly altered by hypoxia; TER decreased and CPP increased in a time- and concentration-dependent manner. Significant alterations in TJ protein expression and increases in HIF1 α and VEGF expression were observed in hypoxic cells, and these effects were attenuated by pretreatment with YC-1. Moreover, corresponding changes in TJ protein expression were also detected in preeclamptic placentas.

Conclusion: These data demonstrate that trophoblast cells undergo significant changes in TJ protein expression under hypoxic conditions and highlight the potential significance of the HIF1 α -VEGF axis in the regulation of TJ structure and function in the preeclamptic placenta.

1. Introduction

The placental syncytium is a critical structure that facilitates the transfer of materials between the mother and developing fetus. The placental barrier is composed of syncytiotrophoblast (ST) cells, cytotrophoblast (CT) cells, vascular endothelial cells, the basement membranes and connective tissues of both the mother and fetus. Damage to or alteration of this barrier is often observed in preeclampsia (PE) and other pregnancy-related complications [1].

Tight junctions (TJs) are junction complexes located at the border of neighboring epithelial cells and formed by transmembrane proteins and

membrane-associated accessory proteins. The transmembrane protein families claudin (CLDN) and occludin (OCLN) contain multiple transmembrane domains and function as homodimeric bridges between adjacent cells [2]. Zonular occludens (ZO) are important membrane-associated accessory proteins that link the cytoplasmic tails of CLDN/OCLN and the actin cytoskeleton to keep the TJs stable. TJs work as both a seal and a “fence”, with the former regulating the paracellular passage/transport of ions and molecules [3] and the latter blocking the movement of membrane molecules between the apical and basolateral domains of the cell plasmalemma. TJs form a major barrier in epithelial tissues and maintain the unique electroosmotic gradients and secretory

Abbreviations: ANOVA, analysis of variance; BSA, bovine serum albumin; CLDN, claudin; CoCl₂, cobalt chloride; CPP, cell paracellular permeability; CT, cytotrophoblast; DMSO, dimethyl sulfoxide; ELISA, enzyme-linked immunosorbent assay; FBS, fetal bovine serum; FITC, fluorescein isothiocyanate; HIF1 α , hypoxia-inducible factor 1 alpha; IF, immunofluorescence; IHC, immunohistochemistry; OCLN, occludin; PBS, phosphate-buffered saline; PE, preeclampsia; qRT-PCR, quantitative reverse-transcription polymerase chain reaction; ST, syncytiotrophoblast; TEM, transmission electron microscopy; TER, transepithelial electrical resistance; TJs, tight junctions; YC-1, 3-(5'-hydroxymethyl-2'-furyl)-1-benzylindazole; ZO, zonular occludens

* Corresponding author.

E-mail address: jyliu_nj@126.com (J.-y. Liu).

¹ These authors contributed equally to this study.

<https://doi.org/10.1016/j.cca.2017.12.010>

Received 14 October 2017; Received in revised form 22 November 2017; Accepted 5 December 2017

Available online 06 December 2017

0009-8981/ © 2017 Published by Elsevier B.V.

paracellular fluids within each type of epithelium. TJs have been well studied in many tissues and cell types. In the placenta, expression of TJ proteins and their locations have been described. CLDN1, CLDN5 and ZO1 were found in human placental vascular trees [4,5] and CLDN4, CLDN16 at the border between the syncytiotrophoblast and cytotrophoblast layers [5]. Our laboratory investigated TJ architecture in placental trophoblasts and vascular endothelial cells using transmission electron microscopy (TEM) [6].

Normal placental function relies on the integrity of TJs. Defects in TJ structures may underlie abnormal placental permeability and contribute to pathological conditions, such as PE. TJs damage was reported in placentas associated with PE, and the expression of some TJ proteins (CLDN1, CLDN3 and CLDN5) were decreased in preeclamptic placentas [5]. Moreover, a study using a co-culture model of placental trophoblasts and endothelial cells further demonstrated alterations of paracellular permeability in preeclamptic placentas [7]; these data strongly suggest the significance of TJ protein dysregulation in the development of PE.

The regulation of TJ expression in placental cells is unclear. Oxygen saturation is crucial for placentation and for supporting normal pregnancy. Hypoxia in the fetal-placental unit has been recognized as a pathological change characteristic of PE [8,9]. It is widely believed that persistent placental hypoxia due to shallow trophoblast invasion and a lack of spiral artery remodeling upregulates HIF-1 α , which leads to endothelial dysfunction and the maternal syndrome of PE [10]. However, how this placental hypoxia leads to the clinical manifestations of PE remains open for debate. Studies of other barrier tissues, such as the blood-brain barrier [11] and the blood-air barrier in the lungs [12], have shown that hypoxia affects TJ protein expression, resulting in impaired TJ functions. Accordingly, we hypothesized that there might be a correlation between hypoxia and TJ dysfunction in the human placental barrier, which may play a role in the pathophysiology of PE. The aim of the present study was to elucidate the effects of hypoxia on the expression of TJ proteins in preeclamptic placentas and BeWo choriocarcinoma cells and to determine whether this regulation of TJs by hypoxia is mediated by hypoxia-inducible factor 1 alpha (HIF1 α).

2. Materials and methods

2.1. Materials

BeWo cells were provided by the China Center for Type Culture Collection. Placental tissues from both PE and control patients were provided by the Clinic Center of Reproductive Medicine of Jiangsu Province Hospital. All subjects provided informed consent, and the research program was approved by the Ethical Committee of the First Affiliated Hospital of Nanjing Medical University. All the placentas were donated by women who had been diagnosed with severe PE during their pregnancies ($n = 10$) or women with normal pregnancies ($n = 7$). All these women had singleton pregnancies, and the babies were delivered by Caesarian section. Clinical data were collected from the Jiangsu Province Hospital Center of Clinical Reproductive Medicine database. Placental specimens were matched based on parity, maternal age, and infant sex (Table 1).

The primary antibodies used were as follows: rabbit anti-ZO1 antibody (Invitrogen, Carlsbad, CA, Catalog No. 61-7300), rabbit anti-HIF1 α antibody (Bioworld, Catalog No. BS3514), rabbit anti-CLDN8 antibody (Sigma Aldrich, St. Louis, MO, Catalog No. AV33621), mouse anti-CLDN4 antibody (Invitrogen, Carlsbad, CA, Catalog No. 32-9400), rabbit anti-OCN antibody (Invitrogen, Carlsbad, CA, Catalog No. 71-1500) and rabbit anti-GAPDH antibody (Bioworld, Catalog No. AP0063). CoCl₂ was purchased from Sigma (St. Louis, MO, USA, Catalog No. C8661). 3-(5'-Hydroxymethyl-2'-furyl)-1-benzylindazole (YC-1) was purchased from Cayman (Ann Arbor, MI, USA, Catalog No. 81560), and fluorescein isothiocyanate (FITC)-dextran was obtained from Sigma (St. Louis, MO, USA, Catalog No. FD4). All chemical

reagents used in our study were at least analytical grade.

2.2. Cell culture and hypoxia model establishment

BeWo cells were maintained at 37 °C as monolayers in F-12 K medium supplemented with 10% fetal bovine serum (FBS), 100 U/ml penicillin and 100 U/ml streptomycin in a humidified atmosphere of 5% CO₂ and 95% air. The cells were subcultured by treatment with 0.25% trypsin containing 0.02% EDTA and then seeded at a density of 3×10^5 cells per well and grown for subsequent experiments. The culture medium was replaced every 24–48 h. Once the cells had reached 70–80% confluence, agents, such as CoCl₂ and/or YC-1 (an inhibitor of HIF1 α expression), were added to the medium. The cells were incubated for the indicated times. Specifically, the *in vitro* cell model of hypoxia was established as follows. BeWo cells were seeded in pore plates or Millicell wells, as required, and then treated with various concentrations (0 μ mol/L, 125 μ mol/L, 250 μ mol/L and 500 μ mol/L) of CoCl₂ or 250 μ mol/L CoCl₂ for various times (6 h, 12 h and 24 h). YC-1 was added to the medium 30 min before treatment with 250 μ mol/L CoCl₂. CoCl₂ was dissolved in F-12 K medium, and YC-1 was dissolved in dimethyl sulfoxide (DMSO).

2.3. TEM examination

The TJ structures of the placenta or BeWo cells were examined using TEM. The placental samples or Millicell membranes on which the cells were cultured were fixed in 2.5% glutaraldehyde in cacodylate buffer. Then, the samples were transferred to cacodylate buffer with 0.05 M sucrose (pH 7.2) and stored at 4 °C. The placental villous tissues or BeWo cells were postfixed in 1% OsO₄ for 2 h at 4 °C and routinely processed in a graded series of acetone. The samples were infiltrated with acetone-araldite and embedded in araldite. The embedding blocks were then cut into semi-thin sections (thickness, 1 μ m) and stained with thionine. The ultrathin sections (thickness, 80 nm) were treated (double contrast) with uranyl acetate for 25 min and 8% lead nitrate for 5 min. The TJ structures of all tissues and cells were systematically investigated at 6,000 \times , 20,000 \times , and 50,000 \times magnification using a JEM-1010 electron microscope (JEOL Ltd.).

2.4. Immunofluorescence (IF)

Cellular localization of proteins of interest was determined by indirect IF. BeWo Cells were grown on sterile glass cover slips, rinsed three times with ice-cold phosphate-buffered saline (PBS), fixed for 30 min in 4% formaldehyde in PBS, and permeabilized for 5 min in PBS containing 0.1% Triton X-100 at room temperature. After being washed, the cells were blocked in 1% bovine serum albumin (BSA)-PBS for 1 h at room temperature. Primary antibodies were diluted to the appropriate concentration in 1% BSA (1:50 dilution) and incubated overnight with the samples at 4 °C. The dilutions for the primary antibodies used in the study are given in Supplemental data 1. The DNA dye Hoechst 33,258 was used for nuclear staining (0.5 mg/ml, permeabilized for 5 min). All washing steps were performed with PBS. Slides were observed under an Axioskop 2 Plus microscope (Carl Zeiss) and photographed.

2.5. Assay of cell paracellular permeability (CPP)

For the cell permeability assay, the cell culture insert system was used, and movement of a macromolecule, FITC-dextran, was assessed. First, BeWo cells (3×10^5) were seeded onto cell culture inserts. When the cultured cells reached 70–80% confluence, FITC-dextran (1 mg/ml, 50 μ L; average molecular mass, 43,200 Da) was added into the upper compartment. CoCl₂ was then added, and the cells were incubated in the absence or presence of YC-1. At the indicated time points, 50 μ L of sample medium was taken from the lower compartment. After diluting

Table 1
Clinical characteristics of placental samples (N = 7 + 10).

	Control (N = 7)	PE (N = 10)
Maternal age (years)	28.86 ± 0.72	28.4 ± 2.63
Nulliparous (N)	6	7
Gestational weeks at delivery	39.5 ± 0.78	37.6 ± 0.79
Mode of delivery	Cesarean	Cesarean
Birth weight (g)	3588.6 ± 199.8	2991.0 ± 516.6
Infant sex		
Female	4	4
Male	3	6

Cases	Age (years)	Gravidity	Parity	Gestational weeks at delivery	Mode of delivery	Sex of the baby	Birth weight (g)	Average systolic BP (at admission)	Average diastolic BP (at admission)	Proteinuria (grams per 24 h urine)
PE1	28	1	0	37.0	Cesarean	Male	2950	160	110	224
PE2	31	4	1	38.3	Cesarean	Male	2800	170	105	335
PE3	33	2	1	39.2	Cesarean	Female	4410	170	110	360
PE4	32	2	0	36.6	Cesarean	Female	2700	190	130	510
PE5	26	1	0	37.1	Cesarean	Female	2900	175	115	210
PE6	27	3	0	37.2	Cesarean	Male	3000	180	110	320
PE7	26	1	0	38	Cesarean	Male	2850	165	110	290
PE8	26	3	1	37.6	Cesarean	Female	3000	170	120	480
PE9	27	1	0	36.9	Cesarean	Male	2600	170	110	360
PE10	28	1	0	38	Cesarean	Male	2700	180	120	510

the sample medium to 500 µL with PBS, the fluorescence intensity of FITC-dextran was measured at excitation and emission wavelengths of 490 nm and 520 nm, respectively, using a fluorescent reader (Spectra MAX Gemini XS).

2.6. Measurement of transepithelial electrical resistance (TER)

The TER of the cell culture insert system was measured using the Millicell ESR apparatus (Millipore corporation, Catalog No. 00198103). BeWo cells were seeded onto Millicell hanging cell culture inserts (diameter, 10 mm; pore size, 0.4 µm; polycarbonate membrane, Millipore corporation, Catalog No. P90740) at a density of 3×10^5 cells per well and then treated as indicated. An equal volume of culture medium without cells served as the blank control. After treatment for the indicated times, the TER of the monolayer of cells was measured. The measurement was performed at a constant temperature (25 °C), and each well was measured three times from 3 different directions. The value of TER was calculated as follows: (the TER value of samples with cells – the TER value of the blank control) \times 0.33.

2.7. Quantitative reverse-transcription polymerase chain reaction (qRT-PCR)

qRT-PCR was performed for quantitative assessment of the mRNA levels of TJ-associated genes, including ZO1, CLDN4, CLDN8, OCLN and VEGF. Total RNA was extracted from cells treated with CoCl_2 and/or 10 µM YC-1 using the RNAiso Plus reagent (TaKaRa Biotechnology Co., Ltd., Dalian, China, TaKaRa code: D9108B) according to the manufacturer's instructions. The first-strand complementary synthesis reaction was performed using a PrimeScript RT Reagent Kit (Perfect Real Time; TaKaRa Biotechnology Co., Ltd., Dalian, China). Gene-specific primers were used, and the sequences are listed in Table 2. GAPDH, a housekeeping gene, was used for normalization. Amplification was conducted using an ABI Prism 7300 Sequence Detection System (PerkinElmer Applied Biosystems, CA). The relative abundances of the target mRNAs were calculated using the $2^{-\Delta\Delta\text{CT}}$ method.

2.8. Western immunoblotting

Cells were collected and boiled in Laemmli sample buffer containing 100 mM dithiothreitol. Proteins were separated by sodium dodecyl

Table 2
Primers used for qRT-PCR.

Gene	Primer	Sequence(5'~3')	Size (bp)
ZO1	Forward	CCAGCCTGCTAACCTACTAAAGTCA	273 bp
	Reverse	TTCATAGCGTAGCCCGTTCAT	
CLDN4	Forward	CTTATGGTGATAGTGCCGGTGTC	197 bp
	Reverse	GCGGAGTAAGGCTTGTCTGTG	
CLDN8	Forward	GATTCCTGCTGGCTCTTCTC	151 bp
	Reverse	TGTGAGCCTTACCTTCTCATTGT	
OCLN	Forward	CTAGGACGCAGCAGATTGGTTTA	153 bp
	Reverse	GGTGATAATGATTGCGTTTGAAT	
VEGF	Forward	AGCAAGACAAGAAAATCCCTGTGG	160 bp
	Reverse	TGGCTTGTACATCTGCAAGTAC	
GAPDH	Forward	GAAGGTCGGAGTCAACGGATTT	223 bp
	Reverse	CTGGAAGATGGTGATGGGATTTTC	

polyacrylamide electrophoresis (SDS-PAGE) and then transferred to nitrocellulose membranes. Primary antibodies, which were diluted in 5% skim milk, were added, and the membranes were incubated overnight at 4 °C. The membranes were washed in PBS before incubation with HRP-conjugated secondary antibodies (1:1000; Zhongshan Biotechnology Co. Ltd., Beijing, China) for 1 h in a hybridization oven at 37 °C. After washing with PBS, the membranes were examined using an enhanced chemiluminescence system (Amersham Biosciences, Uppsala, Sweden). The membranes were then scanned, and the signal intensity of each band was determined using Alpha Ease FC (Fluorchem 5500) software (Alpha Innotech Corp., CA). To standardize for loading variations, the relative protein expression levels in each sample were normalized to GAPDH.

2.9. Enzyme-linked immunosorbent assay (ELISA)

The levels of immunoreactive VEGF in the conditioned supernatant were measured with a commercial ELISA kit, according to the instructions provided by the manufacturer. This assay has a sensitivity of 5.0 pg/mL, with intraassay and interassay coefficients of variation of 10%. The expression levels of VEGF were measured at an emission wavelength of 450 nm with a fluorescent reader (Spectra MAX Gemini XS). The ELISA results were normalized for protein content, and the data are expressed as picograms per milliliter of conditioned medium per microgram of protein.

2.10. Immunohistochemistry (IHC)

To investigate the functions of TJ-related proteins in PE, IHC was performed to analyze differences in the levels of ZO1, CLDN4, CLDN8 and OCLN between PE and normal placentas. Formalin-fixed, paraffin-embedded placental tissues from the control and PE groups were deparaffinized, re-hydrated, sectioned (4 μm) and immunostained. Detection of these proteins in placental tissues was carried out by two-step IHC. Primary antibodies were incubated at a specific concentration overnight at 4 $^{\circ}\text{C}$. The primary antibodies utilized are shown in the Supplemental Table (see Supplemental data 1). Secondary antibodies were incubated at a 1:500 dilution for 1 h at 37 $^{\circ}\text{C}$. IgG was used as the negative control. IHC staining of the placental samples and negative controls was conducted simultaneously using the same methods.

2.11. Statistical analyses

All data are presented as the mean \pm SEM. Comparisons between the study and control groups were calculated by an unpaired *t*-test or one-way analysis of variance (ANOVA), as indicated. Differences were considered statistically significant at a value of $p < 0.05$.

3. Results

3.1. TJ structure and expression of tight junction proteins in human placenta and trophoblast cells

To observe the location of TJ structures in human placenta and trophoblast cells, microscopic observation was performed. As shown in Fig. 1, in human placentas, TJs were mainly located at the cell junctions of adjacent syncytiotrophoblast cells located on the top of the free surface (Fig. 1, A) and at cell junctions with the endothelium (see

Supplemental data 1). In cultured trophoblast cells, TJs were located at the cell-cell junctions. The cellular location of ZO1 and CLDN8 in human placenta was evaluated using IHC (Fig. 1, B). ZO1 and CLDN8 were mostly located in the cytoplasm of syncytiotrophoblasts. Immunofluorescence was conducted to identify the subcellular location of TJ proteins, including ZO1, CLDN4, CLDN8 and OCLN (Fig. 1, D). ZO1 was principally located in the cell junction, and most OCLN molecules were located in the cytoplasm, with a lower level detected in the cell junction and endonuclear regions. CLDN4 and CLDN8 were mainly located in the cytoplasm.

3.2. Increased cell CPP and decreased TER in response to CoCl_2 -induced hypoxia in BeWo cells

To access TJ function under hypoxia, the CPP levels were quantified by measuring FITC-dextran flux through the paracellular monolayers in the Millicell culture system after CoCl_2 treatment. A dose- and time-dependent increase in CPP was observed (Fig. 2A1). While treatment with 125 $\mu\text{mol/L}$ CoCl_2 did not alter the CPP levels of BeWo cells, exposure to 250 $\mu\text{mol/L}$ or 500 $\mu\text{mol/L}$ CoCl_2 caused a significant change in CPP levels. The time course study showed a maximal effect following 24 h of CoCl_2 treatment. TER was measured with a Millicell ESR apparatus. Again, dose- and time-dependent decreases of TER were observed when BeWo cells were treated with CoCl_2 (Fig. 2A2). Similar to the effect of CPP, no significant alteration of TER was detected following treatment with 125 $\mu\text{mol/L}$ CoCl_2 for the three time points examined, while a significant decrease of TER was observed following treatment with 250 or 500 $\mu\text{mol/L}$ CoCl_2 . To confirm that the alterations of CPP and TER were not due to cytotoxicity, cell viability was assessed with the MTT assay (see Supplemental data 2). At dosages of 125 $\mu\text{mol/L}$ and 250 $\mu\text{mol/L}$, no significant difference in cell viability was observed. However, treatment with 500 $\mu\text{mol/L}$ CoCl_2 resulted in

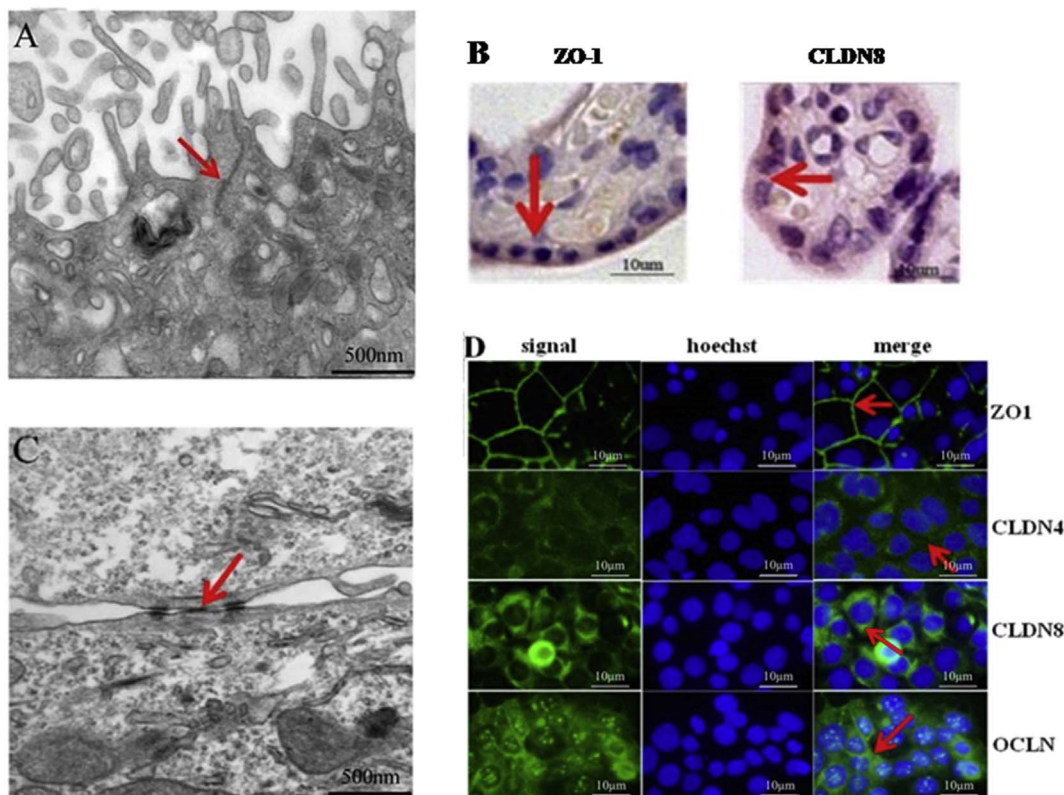


Fig. 1. Location of tight junction (TJ) structures and proteins in human placenta and trophoblast cells. The TJ structures of human placenta (A) and BeWo cells (C) growing on the Millicell membrane were observed with TEM at 50,000 \times magnification (scale bar, 500 nm). The cellular location of ZO1 and CLDN8 in human placenta was determined with the use of IHC (scale bar, 10 μm) (B). The cellular localization of ZO1, CLDN4, CLDN8 or OCLN in BeWo cells was determined with immunofluorescence. (Scale bar = 10 μm) (D).

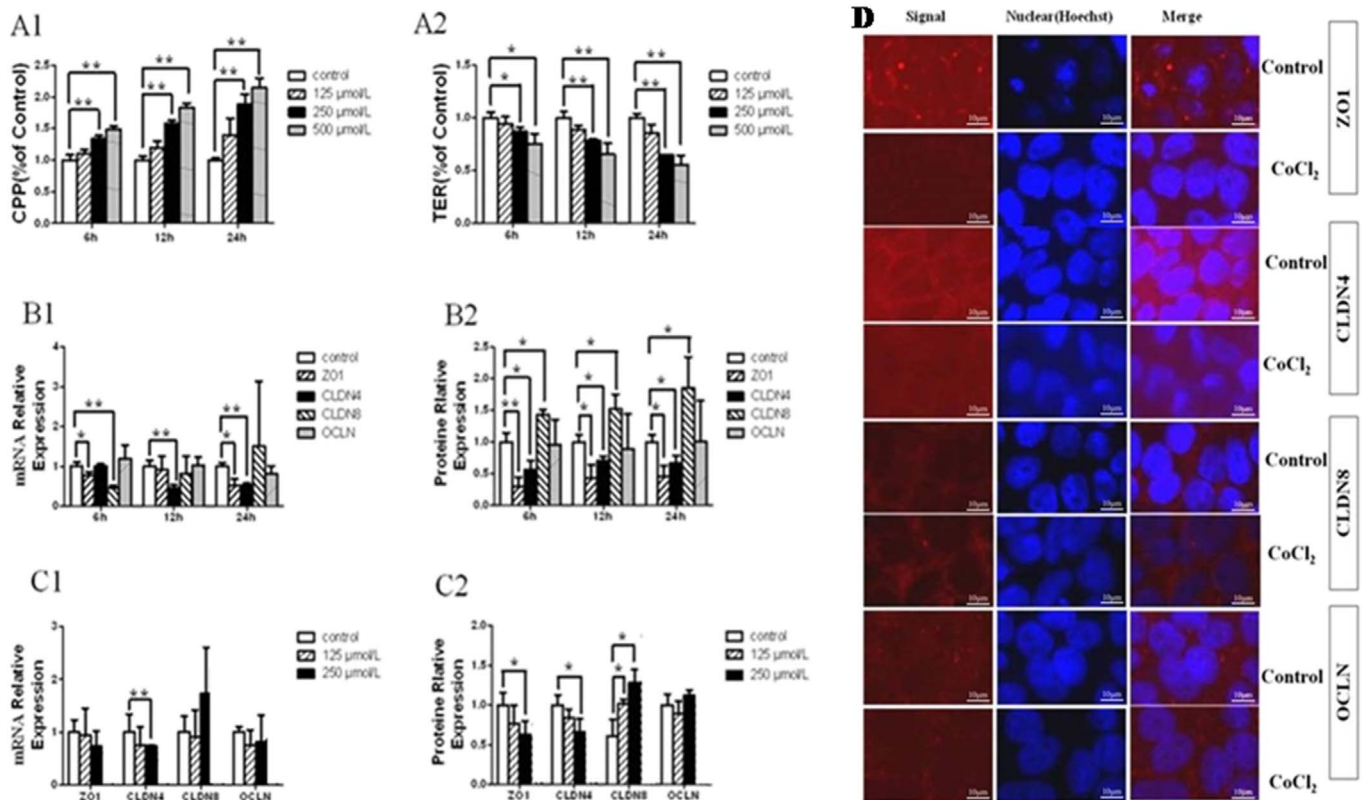


Fig. 2. Dysfunction and alterations of tight junction protein expression in response to the CoCl₂-induced hypoxic condition. BeWo cells cultured in the Millicell culture system were exposed to various concentrations (control, 125 μmol/L, 250 μmol/L and 500 μmol/L) of CoCl₂. At the indicated time points (6 h, 12 h, and 24 h), the leakage of FITC-dextran through the Millicell membrane was measured (A1). TER between the membranes was measured with an ESR apparatus (A2). After exposure to 250 μmol/L CoCl₂ for the indicated times, the mRNA (B1) and protein (B2) expression levels of ZO1, CLDN4, CLDN8 and OCLN were measured by qRT-PCR and Western blotting, respectively. A dose-dependent effect on the expression levels of ZO1, CLDN4, CLDN8 and OCLN was measured both at the mRNA (C1) and protein (C2) levels. After exposure to 250 μmol/L CoCl₂ for 24 h, the locations of ZO1, CLDN4, CLDN8 and OCLN were visualized by immunofluorescence (D). The data represent the mean ± S.E.M. from three independent experiments. *, $p < 0.05$, compared to the control group at each time point. **, $p < 0.01$, compared to the control group at each time point.

apparent cytotoxicity in BeWo cells, and cell viability was greatly reduced. Thus, we used the concentrations of 125 μmol/L and 250 μmol/L in the subsequent experiments to assess the influence of different CoCl₂ concentrations on the expression of TJ proteins in trophoblast cells.

3.3. Alterations of tight junction protein expression in response to CoCl₂-induced hypoxia

To determine whether the CoCl₂-induced functional changes in the TJ barrier were associated with alterations in the expression of TJ proteins, the mRNA and protein levels of ZO1, CLDN4, CLDN8 and OCLN were measured with qRT-PCR and Western blotting. As shown in Fig. 2B1, following treatment with 250 μmol/L CoCl₂, ZO1 mRNA expression levels were reduced at 6 h and 24 h, while CLDN4 mRNA levels were significantly reduced at 12 h and 24 h. CLDN8 showed a low level of expression at 6 h, and no statistically significant difference was observed between the two groups at 12 h or 24 h. We also measured the expression of OCLN mRNA and found no significant difference between the treated and untreated cells at any time points analyzed.

We assessed how the protein levels of these TJ proteins changed in response to treatment with 250 μmol/L CoCl₂. A marked reduction of ZO1 and CLDN4 was detected in the treated cells at 6 h, 12 h and 24 h compared with the levels in untreated cells (Fig. 2B2). In contrast, the expression of CLDN8 was significantly elevated, while the expression of OCLN was not affected (Fig. 2B2). These results at the protein level were consistent with those observed at the mRNA level.

The dose-dependent responses to CoCl₂ treatment were also determined. While there was a trend of reduction in the ZO1 mRNA level

following treatment with 125 μmol/L or 250 μmol/L CoCl₂ for 12 h, the change did not reach statistical significance (Fig. 2C1). However, on the protein level, treatment with 250 μmol/L CoCl₂ led to a significant reduction of ZO1 (Fig. 2C2). CLDN4 expression was decreased at both the mRNA and protein levels after the treatment with 250 μmol/L CoCl₂ but not at the 125 μmol/L CoCl₂ concentration (Fig. 2C1 and C2). mRNA levels of CLDN8 showed no statistically significant difference among the different concentration groups (Fig. 2C1), whereas on the protein level, there was a significant increase in CLDN8 expression at both the 125 μmol/L and 250 μmol/L concentrations (Fig. 2C2). No evident change in OCLN expression was found following treatment with different concentrations of CoCl₂ (Fig. 2C1 and C2).

To examine the potential location alteration of TJ proteins under hypoxia, the distribution of TJ proteins was observed under a fluorescence microscope. The results showed no obvious location alterations for ZO1, CLDN4, CLDN8 and OCLN after treatment with 250 μmol/L CoCl₂, although the changes in the expression levels of ZO1, CLDN4, and CLDN8 were consistent with the Western blotting results.

3.4. HIF1α and VEGF contribute to TJ dysfunction under the response to CoCl₂-induced hypoxia

We determined HIF1α and VEGF expression changes induced by hypoxia in BeWo cells. As seen in Fig. 3A1, elevated HIF1α expression was detected in a time-dependent manner after exposure to 250 μmol/L CoCl₂ in Western blotting experiments. While no change in HIF1α expression was observed at the 125 μmol/L concentration, a significant change was detected after treatment with 250 μmol/L CoCl₂ (Fig. 3A2). Using an ELISA kit, the protein concentration of VEGF in culture media

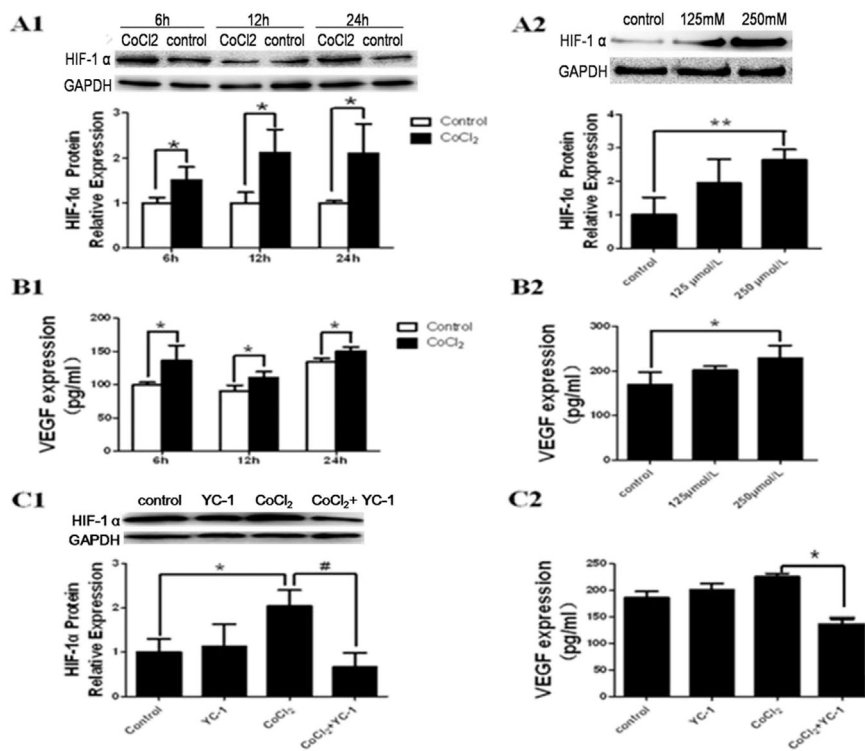


Fig. 3. Alterations in HIF1 α and VEGF expression in response to CoCl₂-induced hypoxia. After the exposure of BeWo cells to 250 μ mol/L CoCl₂ for the indicated times (6 h, 12 h, and 24 h), the protein expression levels of HIF1 α (A1) and VEGF (B1) were assessed with Western blotting and ELISA, respectively. Following exposure to different concentrations of CoCl₂ (125 μ mol/L and 250 μ mol/L) for 12 h, the protein expression levels of HIF1 α (A2) and VEGF (B2) were measured. The BeWo monolayer culture was pretreated with the HIF1 α inhibitor YC-1. Following 250 μ mol/L CoCl₂ treatment, the protein expression levels of HIF1 α (C1) and VEGF (C2) were assessed. The data represent the mean \pm S.E.M. from three independent experiments. *, $p < 0.05$, compared to the control group at each time point. **, $p < 0.01$, compared to the control group at each time point.

was measured. Similarly, a time-dependent increase of VEGF at 250 μ mol/L CoCl₂ was observed (Fig. 3B1 and B2).

We applied the HIF1 α inhibitor, YC-1, to verify the HIF1 α regulation on VEGF. BeWo cells were pretreated with YC-1 before CoCl₂ treatment. YC-1 treatment alone significantly reduced HIF1 α and VEGF expression (Fig. 3C1 and C2), confirming the efficacy of YC-1 as a HIF1 α inhibitor. Importantly, pretreatment with YC-1 blocked the cell response to CoCl₂, indicating that in the HIF1 α -VEGF pathway, the VEGF changes caused by CoCl₂ exposure are mostly mediated by HIF1 α . Subsequently, we determined the role of HIF1 α in the regulation of TJ protein under hypoxia. As shown in Fig. 4, HIF1 α inhibition by YC-1 (10 μ mol/L) significantly reversed the elevation in CPP (Fig. 4A) and decrease in TER (Fig. 4B) induced by CoCl₂. Moreover, while the protein levels of ZO1 and CLDN4 were reduced by CoCl₂ exposure for 24 h, these effects were blocked by pretreatment with the HIF1 α inhibitor. In parallel, CoCl₂-induced elevation of CLDN8 expression was also blocked by YC-1 pretreatment (Fig. 4C). In addition, immunofluorescence staining results also confirmed that the alterations of TJ protein expression were neutralized by HIF1 α inhibition. Thus, HIF1 α appeared to be a major factor mediating the hypoxia-triggered disruption of TJ functions and dysregulation of TJ protein expression.

3.5. Alteration of tight junction protein expression and HIF1 α in PE placentas

To verify the *in vivo* significance of the above findings in cell culture, the mRNA and protein expression of TJ proteins were examined in preeclamptic placentas. As shown in Fig. 5A and B, decreased expression levels of ZO1 and CLDN4 were detected in PE placentas at both the mRNA and protein levels compared to those in placentas from normal pregnancies. The expression of CLDN8 was increased in preeclamptic placentas compared with that in normal placentas, while no difference in OCLN expression was observed (Fig. 5A and B). Using IHC, we compared the location and expression of ZO1 and CLDN8 in preeclamptic and normal placentas (Fig. 5D). ZO1 and CLDN8 were mainly localized in the cytoplasm of syncytiotrophoblasts. No alteration in the location of these TJ proteins was detected in PE placentas, while ZO1

protein expression was decreased and CLDN8 protein was increased compared to the levels in normal placentas. Thus, the altered expression of TJ proteins in PE placentas was similar to that observed in trophoblast cells induced by hypoxia, indicating that hypoxia-induced TJ dysfunction may be involved in the pathogenesis of PE. Moreover, we assessed HIF1 α expression in PE and control placentas and found a significant elevation of HIF1 α expression in PE (Fig. 5C and D). Thus, hypoxia may contribute to the development of PE via the HIF1 α pathway.

4. Discussion

The placental barrier serves as the frontline defense to protect the fetus. Specifically, this barrier controls the transport of ions, solutes and water across the epithelia through both transcellular and paracellular passages. Maintenance of the concentration gradients in the nutrients and wastes across placental barriers is dependent on the integrity of TJs between adjacent cells [13]. Trophoblast cells, as one of the most important cell types in the placenta, play a significant role in sustaining the homeostasis of the placental barrier. Dysfunctional TJs in human placenta and trophoblast cells are correlated with abnormal placental functions and the development of pregnancy complications [13–15]. In this study, utilizing a cell culture model, we examined the effects of hypoxia on the TJs of placental trophoblasts. Our results showed that hypoxia significantly modified TJ protein expression and function in BeWo cells, and this effect was most likely mediated by the HIF1 α -VEGF axis. Additionally, in PE placentas, the expression of TJ proteins was significantly altered compared to that in control placentas. Together, the present results provide some novel insights into the mechanism of placental dysfunction.

Although TJs have been widely investigated in other organs and systems, PE-related alterations in TJ structure and function have not been well elucidated. Previous studies have shown that TJ structures and proteins are located both in endothelial cells and trophoblast cells of human placenta [4,5,16,17]. TJ protein expression was found to be altered throughout gestation, indicating that TJs participate in normal placentation. Studies also showed that the destruction of TJ structure

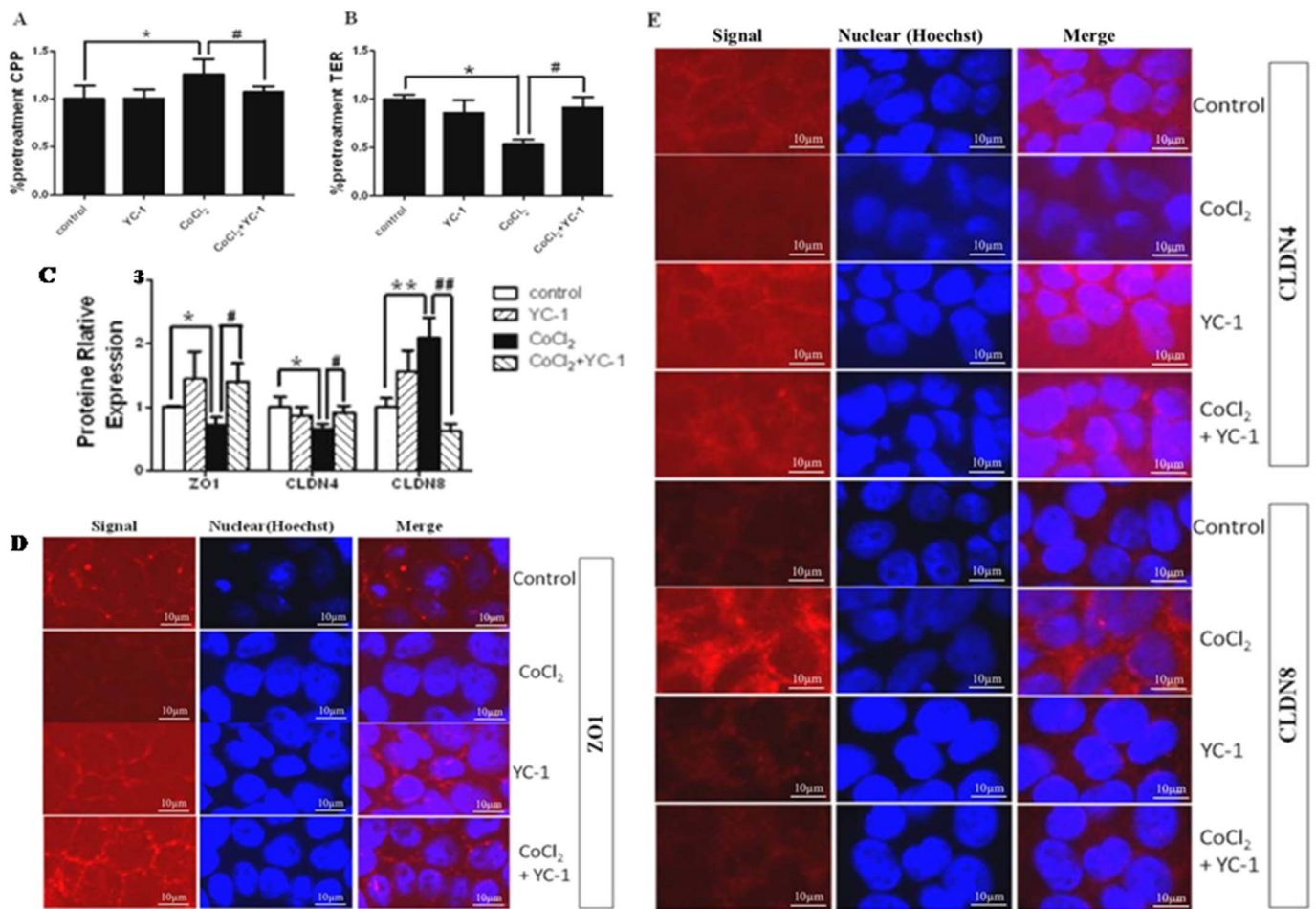


Fig. 4. HIF1 α and VEGF contribute to the regulation of tight junction functions in response to CoCl₂-induced hypoxia. BeWo cells were pretreated with YC-1 (10 μ mol/L) for 30 min in the presence or absence of CoCl₂ (250 μ mol/L) for 24 h before CPP (A) and TER (B) were measured. Meanwhile, the expression of tight junction proteins, including ZO1, CLDN4, and CLDN8 (C), was detected with Western blotting. The cellular localization of ZO1, CLDN4, and CLDN8 was determined with indirect immunofluorescence (D, E). The data represent the mean \pm S.E.M. from three independent experiments. *, $p < 0.05$, compared to the control group. **, $p < 0.01$, compared to the control group. #, $p < 0.05$, compared to the CoCl₂-treated group, ##, $p < 0.01$, compared to the CoCl₂-treated group.

and altered expression of TJ proteins are associated with complete hydatidiform moles [18]. In PE placenta, Samuel Liévano observed the downregulation of CLDN1, CLDN3, and CLDN 5 and an unaltered expression of ZO1 and occludin, but no mechanistic study was performed [5]. Alterations of TJ proteins in PE placentas suggest a dysfunction in the TJ barrier in this condition. As a result, fluxes of macromolecules across the paracellular route may be increased, which might account for the edema of the placenta observed in PE patients. In addition, some investigators have found that reduced TJ expression was accompanied by paracellular leakage when trophoblast cells were cocultured with cytokines derived from PE placentas [7]. Our findings on the ZO1 and CLDN8 changes in BeWo cells under hypoxia, alterations of CPP and TER functions, together with corresponding changes in preeclamptic placentas, has provided additional data in support of hypoxia-induced TJ changes in the development of PE.

Hypoxia has been shown to alter the expression and location of TJ proteins, leading to decreased restrictiveness of the barrier and defective paracellular transport, thereby resulting in epithelium barrier dysfunction [12,19]. Willis et al. [20] observed that in rat brains, hypoxia induced the downregulation of CLDN5, OCLN and ZO1 at the blood-brain barrier. In cultured human corneal epithelial cells, Kimura et al. [21] observed that hypoxia induced the disruption of barrier function and a downregulation of TJ proteins, while dexamethasone exhibited a protective effect on epithelial barrier dysfunction by inhibiting the degradation of ZO1. Again, in non-placental cells, the

HIF1 α -VEGF axis was found to mediate downstream cellular responses to the hypoxia condition [22,23]. As one of the most important downstream target genes of HIF1 α , VEGF is a vascular permeability factor that is particularly important in endothelial cells [24]. Studies on barrier systems have demonstrated the relationship between VEGF and TJs in non-trophoblast cells. In a blood-brain barrier model, Davis et al. [25] found that hypoxia upregulated VEGF expression, which increased blood-brain barrier permeability. Both in brain microvessel endothelial cell cultures and in the central nerve system, Argaw et al. [26] proved that VEGF inhibited CLDN5 and OCLN expression at both the mRNA and protein levels, leading to dysfunction of the brain barrier. Cai et al. [27] found that VEGF induced the downregulation of ZO1 and CLDN5 in retinal cells, thereby resulting in eye damage in mice. However, opposing results have also been reported. Zhou et al. [28] observed that the downregulation of VEGF induced cell barrier impairment of human umbilical vein endothelial cells *in vitro*. Our studies showed that dysfunctional TJs and alterations of TJ protein expression induced by hypoxia is mediated by the HIF1 α -VEGF axis. We speculate that the hypoxia-induced TJ dysfunction in trophoblasts might cause the release of anti-angiogenic factors, such as soluble Fms-like tyrosine kinase-1 (sFLT-1) and soluble endoglin (sENG), into the maternal vasculature, and this is believed to be a crucial step in the pathogenesis of PE [29]. Moreover, YC-1 has been shown to reduce sFLT-1 and sENG secretion from human primary trophoblast cells and placental explants derived from patients with PE, concordant with the downregulation of HIF1 α

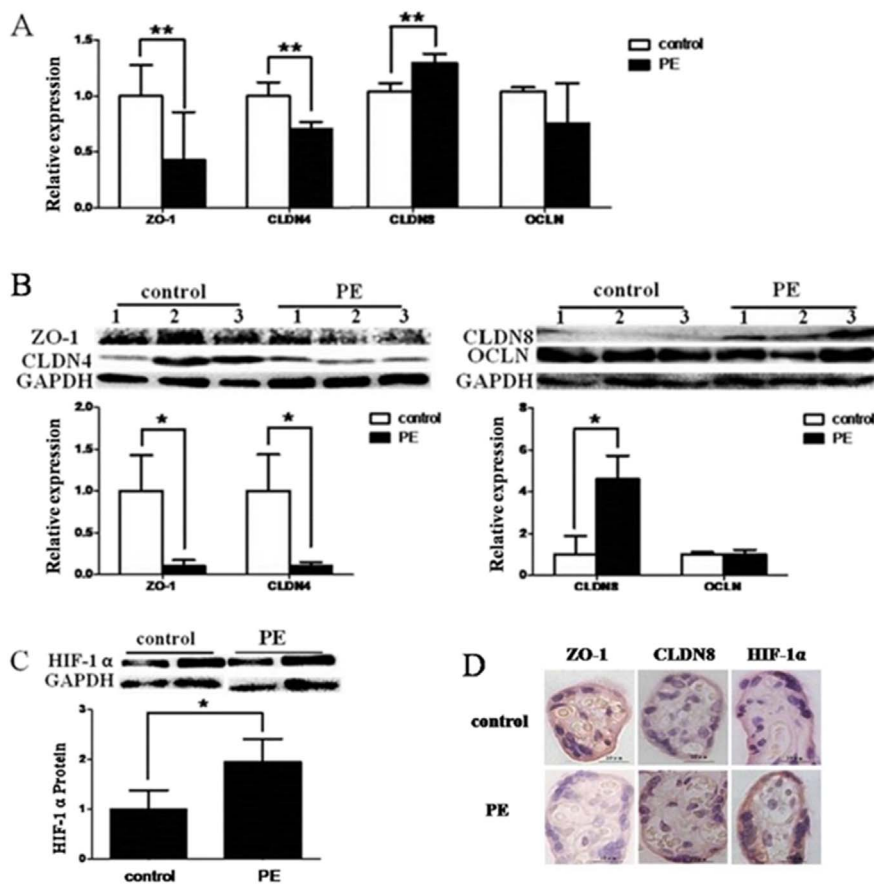


Fig. 5. Altered expression of HIF1 α and tight junction (TJ) proteins in PE placenta. The expression of TJ proteins, including ZO1, CLDN4, CLDN8 and OCLN, in preeclamptic and normal placentas was measured at the mRNA (A) and protein levels (B) with qRT-PCR and Western blotting, respectively. The difference in HIF1 α protein expression between the two groups was assessed by Western blotting (C) and IHC (D). The data represent the mean \pm S.E.M. from three independent experiments. *, $p < 0.05$, compared to the control group. **, $p < 0.01$, compared to the control group.

expression [30]. These data emphasize the significance of hypoxia-induced HIF α and the potential role of VEGF in the development of PE. In our present study, we did not conduct any experiments to elucidate the relation between hypoxia-induced TJ dysfunction and the direct secretion of sFLT-1 and sENG. Further studies on the detailed molecular mechanism of VEGF regulatory pathway leading to the increasing placental permeability are required for a better comprehension of PE pathogenesis.

In summary, our data demonstrate that placental trophoblasts undergo significant changes in TJ protein expression under conditions of CoCl₂-induced hypoxia. The HIF1 α -VEGF axis plays a major role in the regulation of TJ expression and function, as reflected by the changes in CPP and TER. *In vivo* studies demonstrated relevant changes in TJ protein expression patterns in placental tissues from preeclamptic and normal pregnancy placentas. Further research regarding TJs will enrich our knowledge regarding the pathogenesis of preeclampsia, which is expected to facilitate the prevention and treatment of this deadly disease affecting a large number of pregnant women.

Acknowledgments

We thank Prof. Jiahao Sha and Prof. Zuomin Zhou, State Key Laboratory of Reproductive Medicine, for their help with the experimental design and technology use.

Conflicts of interest

The authors declare that they have no conflicts of interest with regard to the contents of this article.

Author contributions

YZ designed the study and wrote the manuscript. HZ and XX acquired the data shown in Figs. 2–5, performed the data analyses and helped write the manuscript. FD, XM and JW helped perform the analyses with constructive discussions. LG, JL and CG helped to acquire the data shown in Fig. 1. YC contributed significantly to analyses and manuscript preparation. JL contributed to the conception of the study and approved the final version. All authors reviewed the results and approved the final version of the manuscript.

Funding resources

This study was supported by The National Key Research and Development Program of China (2017YFC1001602), the National Nature and Science Foundation (81401265, 81401267), Jiangsu Province Programs [BK20141025], and a project from Jiangsu Higher Education Institution (PAPD, JX10231802).

Appendix A. Supplementary data

Supplementary data to this article can be found online at <https://doi.org/10.1016/j.cca.2017.12.010>.

References

- [1] B.C. Young, R.J. Levine, S.A. Karumanchi, Pathogenesis of preeclampsia, *Annu. Rev. Pathol.* 5 (2010) 173–192.
- [2] C. Ahn, H. Yang, D. Lee, B.S. An, E.B. Jeung, Placental claudin expression and its regulation by endogenous sex steroid hormones, *Steroids* 100 (2015) 44–51.
- [3] L. Shen, Tight junctions on the move: molecular mechanisms for epithelial barrier regulation, *Ann. N. Y. Acad. Sci.* 1258 (2012) 9–18.
- [4] L. Leach, M.O. Babawale, M. Anderson, M. Lammiman, Vasculogenesis, angiogenesis and the molecular organisation of endothelial junctions in the early human

- placenta, *J. Vasc. Res.* 39 (2002) 246–259.
- [5] S. Liévano, L. Alarcón, B. Chávez-Munguía, L. González-Mariscal, Endothelia of term human placenta display diminished expression of tight junction proteins during preeclampsia, *Cell Tissue Res.* 324 (2006) 433–448.
- [6] Y. Zhang, N. Zhao, H. Zhao, Y. Cui, J. Liu, Expression of tight junction factors in human placental tissues derived from assisted reproductive technology and natural pregnancy, *Zhonghua Fu Chan Ke Zhi* 49 (2014) 125–129.
- [7] Y. Wang, Y. Gu, Y. Zhang, D.F. Lewis, Evidence of endothelial dysfunction in preeclampsia: decreased endothelial nitric oxide synthase expression is associated with increased cell permeability in endothelial cells from preeclampsia, *Am. J. Obstet. Gynecol.* 190 (2004) 817–824.
- [8] H.A. Korkeas, L. De Oliveira, N. Sass, S. Salahuddin, S.A. Karumanchi, A. Rajakumar, Relationship between hypoxia and downstream pathogenic pathways in preeclampsia, *Hypertens. Pregnancy* 36 (2017) 145–150.
- [9] X. Guo, L. Feng, J. Jia, R. Chen, J. Yu, Upregulation of VEGF by small activating RNA and its implications in preeclampsia, *Placenta* 46 (2016) 38–44.
- [10] R. Tal, The role of hypoxia and hypoxia-inducible factor-1alpha in preeclampsia pathogenesis, *Biol. Reprod.* 87 (134) (2012) 1–8.
- [11] M. Morin-Brureau, A. Lebrun, M.C. Rousset, et al., Epileptiform activity induces vascular remodeling and zonula occludens 1 downregulation in organotypic hippocampal cultures: role of VEGF signaling pathways, *J. Neurosci.* 31 (2011) 10677–10688.
- [12] J.C. Caraballo, C. Yshii, M.L. Butti, et al., Hypoxia increases transepithelial electrical conductance and reduces occludin at the plasma membrane in alveolar epithelial cells via PKC- ζ and PP2A pathway, *Am. J. Phys. Lung Cell. Mol. Phys.* 300 (2011) L569–L578.
- [13] L.L. Mitic, C.M. Van Itallie, J.M. Anderson, Molecular physiology and pathophysiology of tight junctions I. Tight junction structure and function: lessons from mutant animals and proteins, *Am. J. Physiol. Gastrointest. Liver Physiol.* 279 (2000) G250–G254.
- [14] M. Harada, M. Kondoh, A. Masuyama, et al., Effect of forskolin on the expression of claudin-5 in human trophoblast BeWo cells, *Pharmazie* 62 (2007) 291–294.
- [15] Y. Zhang, Y. Cui, Z. Zhou, J. Sha, Y. Li, J. Liu, Altered global gene expressions of human placenta subjected to assisted reproductive technology treatments, *Placenta* 31 (2010) 251–258.
- [16] L. Leach, M.J. Lammiman, M.O. Babawale, et al., Molecular organization of tight and adherens junctions in the human placental vascular tree, *Placenta* 21 (2000) 547–557.
- [17] T. Wang, J. Schneider, Cellular junctions on the free surface of human placental syncytium, *Arch. Gynecol.* 240 (1987) 211–216.
- [18] D. Marzioni, M. Banita, A. Felici, et al., Expression of ZO-1 and occludin in normal human placenta and in hydatidiform moles, *Mol. Hum. Reprod.* 7 (2001) 279–285.
- [19] C.M. Zehendner, L. Librizzi, M. de Curtis, C.R. Kuhlmann, H.J. Luhmann, Caspase-3 contributes to ZO-1 and Cl-5 tight-junction disruption in rapid anoxic neurovascular unit damage, *PLoS One* 6 (2011) e16760.
- [20] C.L. Willis, D.S. Meske, T.P. Davis, Protein kinase C activation modulates reversible increase in cortical blood-brain barrier permeability and tight junction protein expression during hypoxia and posthypoxic reoxygenation, *J. Cereb. Blood Flow Metab.* 30 (2010) 1847–1859.
- [21] K. Kimura, S. Teranishi, K. Kawamoto, T. Nishida, Protective effect of dexamethasone against hypoxia-induced disruption of barrier function in human corneal epithelial cells, *Exp. Eye Res.* 92 (2011) 388–393.
- [22] H. Guo, H. Zhou, J. Lu, Y. Qu, D. Yu, Y. Tong, Vascular endothelial growth factor: an attractive target in the treatment of hypoxic/ischemic brain injury, *Neural Regen. Res.* 11 (2016) 174–179.
- [23] S. Shiratsuki, T. Hara, Y. Munakata, K. Shirasuna, T. Kuwayama, H. Iwata, Low oxygen level increases proliferation and metabolic changes in bovine granulosa cells, *Mol. Cell. Endocrinol.* 437 (2016) 75–85, <http://dx.doi.org/10.1016/j.mce.2016.08.010>.
- [24] E.E. Gorbunova, I.N. Gavrillovskaia, T. Pepini, E.R. Mackow, VEGFR2 and Src kinase inhibitors suppress Andes virus-induced endothelial cell permeability, *J. Virol.* 85 (2011) 2296–2303.
- [25] B. Davis, J. Tang, L. Zhang, et al., Role of vasodilator stimulated phosphoprotein in VEGF induced blood-brain barrier permeability in endothelial cell monolayers, *Int. J. Dev. Neurosci.* 28 (2010) 423–428.
- [26] A.T. Argaw, B.T. Gurfein, Y. Zhang, A. Zameer, G.R. John, VEGF-mediated disruption of endothelial CLN-5 promotes blood-brain barrier breakdown, *Proc. Natl. Acad. Sci. U. S. A.* 106 (2009) 1977–1982.
- [27] J. Cai, L. Wu, X. Qi, et al., Placenta growth factor-1 exerts time-dependent stabilization of adherens junctions following VEGF-induced vascular permeability, *PLoS One* 6 (2011) e18076.
- [28] Q. Zhou, H. Liu, F. Qiao, Y. Wu, J. Xu, VEGF deficit is involved in endothelium dysfunction in preeclampsia, *J. Huazhong Univ. Sci. Technol. Med. Sci.* 30 (2010) 370–374.
- [29] R. Tal, A. Shaish, I. Barshack, et al., Effects of hypoxia-inducible factor-1alpha overexpression in pregnant mice: possible implications for preeclampsia and intrauterine growth restriction, *Am. J. Pathol.* 177 (2010) 2950–2962.
- [30] F.C. Brownfoot, S. Tong, N.J. Hannan, et al., YC-1 reduces placental sFlt-1 and soluble endoglin production and decreases endothelial dysfunction: a possible therapeutic for preeclampsia, *Mol. Cell. Endocrinol.* 413 (2015) 202–208.